Journal of Alloys and Compounds 509 (2011) 4878–4881

Contents lists available at ScienceDirect

Journal of Alloys and Compounds

journal homepage: www.elsevier.com/locate/jallcom

In situ dynamical control of the strain and magnetoresistance of $La_{0.7}Ca_{0.15}Sr_{0.15}MnO_3$ thin films using the magnetostriction of Terfenol-D alloy

R.K. Zheng[a,*], S.H. Choy[a], Y. Wang[a], H.L.W. Chan[a], C.L. Choy[a], H.S. Luo[b]

[a] Department of Applied Physics and Materials Research Center, The Hong Kong Polytechnic University, Hong Kong, China
[b] State Key Laboratory of High Performance Ceramics and Superfine Microstructure, Shanghai Institute of Ceramics, Chinese Academy of Sciences, Shanghai 201800, China

ARTICLE INFO

Article history:
Received 14 September 2010
Received in revised form 20 January 2011
Accepted 28 January 2011
Available online 4 February 2011

Keywords:
Magnetoelectric effect
PMN–PT single crystal
Magnetoresistance
Terfenol-D magnetostrictive alloy

ABSTRACT

We fabricated a magnetoelectric laminate structure consisting of a magnetostrictive $Tb_{0.3}Dy_{0.7}Fe_{1.92}$ (Terfenol-D) plate bonded to a $La_{0.7}Ca_{0.15}Sr_{0.15}MnO_3$ (LCSMO)/$0.67Pb(Mg_{1/3}Nb_{2/3})O_3$-$0.33PbTiO_3$ (PMN–PT) structure where a LCSMO film was epitaxially grown on a PMN–PT single crystal substrate. When a dc magnetic field is applied perpendicular to the film plane, the magnetoresistance of the LCSMO film in the paramagnetic (ferromagnetic) state for the LCSMO/PMN–PT/Terfenol-D structure is larger (smaller) than that for the LCSMO/PMN–PT structure without Terfenol-D. These effects are caused by the magnetostriction-induced in-plane compressive strain in the Terfenol-D, which are transferred to the PMN–PT substrate, leading to a reduction in the in-plane tensile strain of the epitaxial LCSMO film and thereby modifying the magnetoresistance of the film.

1. Introduction

It has been rather difficult to study and understand the substrate-induced strain effects in complex oxide thin films and the subject continues to be a focus for research [1–5]. To obtain the strain effects in these films, investigators usually grow thin films with different thicknesses on lattice-mismatched substrates before comparing the properties of these strained films. However, in addition to strain, many extrinsic variables such as oxygen content, film crystallinity, microstructural defects and disorders, dead layer at the interface, etc., may also strongly influence the properties of thin films [1–5]. It is therefore difficult to separate the effects of substrate-induced strain from those of extrinsic variables on the properties of thin films.

A number of experimental work [6–9] have demonstrated that the in-plane strain of piezoelectric $(1-x)Pb(Mg_{1/3}Nb_{2/3})O_3$–$xPbTiO_3$ (PMN–*x*PT) single crystals in PMN–*x*PT/Terfenol-D laminate structures can be dynamically modulated by applying a dc/ac magnetic field. This dynamical modulation of the strain of PMN–*x*PT single crystals using magnetic field implies that the strain and properties of complex oxide thin films epitaxially grown on PMN–*x*PT single crystal substrates could be dynamically modified if a film/PMN–*x*PT structure is bonded to a Terfenol-D plate to form a film/PMN–*x*PT/Terfenol-D laminate structure. In this paper, we report that it is possible to modify the strain and magnetoresistance (MR) of a $La_{0.7}Ca_{0.15}Sr_{0.15}MnO_3$ (LCSMO) thin film epitaxially grown on a $0.67Pb(Mg_{1/3}Nb_{2/3})O_3$–$0.33PbTiO_3$ (PMN–PT) single crystal substrate (which has a piezoelectric coefficient d_{33}–1500 pm/V) by changing the magnetostriction of the Terfenol-D plate in a LCSMO/PMN–PT/Terfenol-D laminate structure. We found that the strain induced by the magnetostriction of the Terfenol-D was transferred to the PMN–PT substrate, causing the strain state of the LCSMO film to alter, and eventually leading to a change in the MR of the film.

2. Experimental details

PMN–PT single crystals were grown through a modified Bridgman technique [10]. The single crystals were cut into rectangular plates (10 mm × 2.5 mm × 0.5 mm) with the plate normal in the ⟨0 0 1⟩ crystal direction and polished until the average surface roughness *Ra* was less than 0.6 nm. Such polished single crystals were used as substrates to grow LCSMO films using dc magnetron sputtering. The film deposition was carried out in an argon–oxygen flow with 60% Ar and 40% O_2 at a pressure of 5 Pa and a substrate temperature of 700 °C. During the deposition, the substrate holder rotated slowly in order to reduce the dispersion of film thickness over the whole film. After deposition, the films were *in situ* cooled to room temperature and postannealed in air at 700 °C for 30 min using a rapid thermal processor furnace. The thickness of the films was estimated to be ~40 nm. The surface morphology of the films was studied under an atomic force microscope (Digital Instruments, Nanoscope IV). The rms roughness was ~0.9 nm over a 5 μm × 5 μm area, implying a smooth film surface. Crystallographic characterization of the films was conducted on a Bruker D8 Discover X-ray diffractometer equipped with Cu Kα radiation.

Fig. 1(a) and (b) shows the electrical measurement circuits for the LCSMO/PMN–PT structure and the LCSMO/PMN–PT/Terfenol-D structure, respectively. Here, the thicknesses of the PMN–PT substrate and the Terfenol-D plate are ~0.5 mm and ~1 mm, respectively. A constant current of 5 μA was applied to the thin film through the two top–top gold electrodes using a Keithley 2400 source

* Corresponding author. Tel.: +852 27665692; fax: +852 27661202.
E-mail address: zrk@ustc.edu (R.K. Zheng).

0925-8388/$ – see front matter © 2011 Elsevier B.V. All rights reserved.
doi:10.1016/j.jallcom.2011.01.197

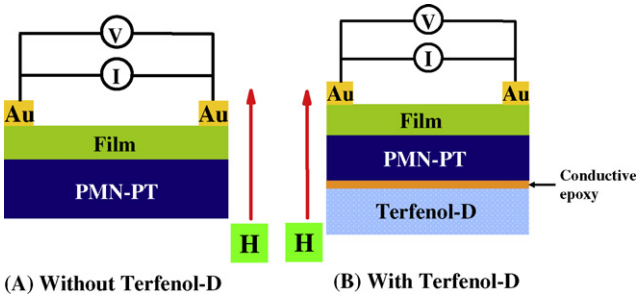

Fig. 1. Schematic diagram and electrical measurement circuits for (a) the LCSMO/PMN–PT structure without Terfenol-D, and (b) the LCSMO/PMN–PT/Terfenol-D structure with Terfenol-D.

meter. The voltage difference between the two top–top gold electrodes was measured using a Keithley 2700 digital multimeter. The MR and magnetic hysteresis loops of the LCSMO films were recorded using a Model 7600 LakeShore Hall/VSM measurement system (LakeShore Cryotronics, Inc. USA).

The magnetoelectric (ME) properties of the LCSMO/PMN–PT/Terfenol-D structure were characterized at room temperature using a home-made automated measurement system [11]. The induced ME voltages between the top gold electrode and the bottom Terfenol-D alloy were measured as a function of ac magnetic field H_{ac} using a 400 MHz WaveRunner oscilloscope (LeCroy Inc. USA). H_{ac} was provided by Helmholtz coils driven by an AFG320 function generator (Sony Tektronix) via constant current Precision Industrial Amplifier (AE Techron Inc. USA). H_{dc} bias field was supplied by a water-cooled electromagnet.

3. Results and discussion

Fig. 2 shows the XRD θ–2θ scan of the LCSMO/PMN–PT structure. The results indicate that the film is preferentially (0 0 l)-oriented and has no secondary phases. The out-of-plane lattice constant is measured to be ~3.848 Å. This value is smaller than that ($c \sim 3.888$ Å [12]) of the LCSMO bulk material, indicating that the film is subjected to an out-of-plane compressive strain and an in-plane tensile strain. The result is consistent with the fact that the lattice constants of the LCSMO bulk materials are smaller than those ($a \sim b \sim c \sim 4.02$ Å [13]) of the PMN–PT single crystals. As shown in Fig. 2(a), the XRD ω-scan rocking curve performed on the LCSMO(002) reflection yields a full width at a half maximum of 0.38°, indicating good crystallinity of the film. We also performed XRD ϕ scans on the LCSMO(1 0 1) and PMN–PT(1 0 1) reflections, respectively, and observed four-fold symmetrical reflections for

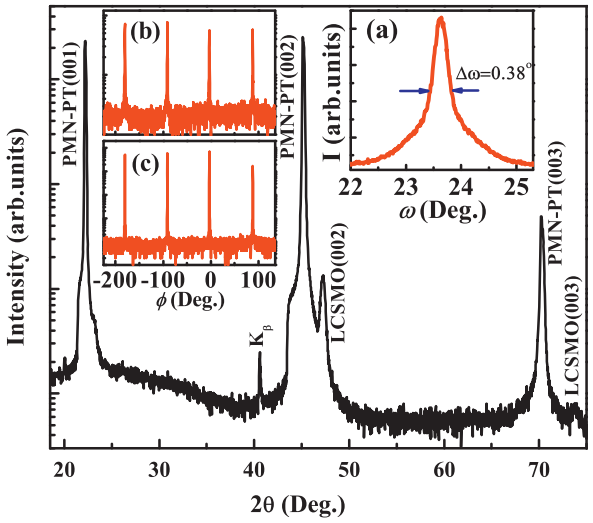

Fig. 2. X-ray diffraction pattern of the LCSMO/PMN–PT structure. Inset (a) shows the ω-scan rocking curve on the LCSMO(002) reflection. Insets (b) and (c) show the XRD ϕ scans on the LCSMO(1 0 1) and PMN–PT(1 0 1) reflections, respectively.

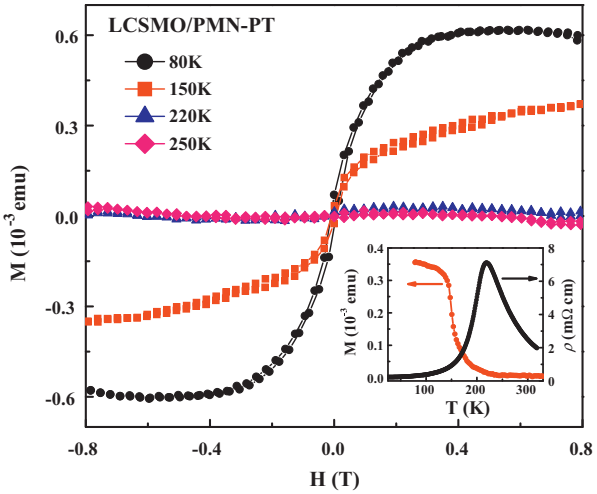

Fig. 3. Magnetic hysteresis loops at T = 80, 150, 220, and 250 K for the LCSMO/PMN–PT structure without Terfenol-D. The inset shows the temperature dependence of the resistivity and the zero-field-cooled magnetization measured at H = 1000 Oe for the LCSMO/PMN–PT structure without Terfenol-D.

both the LCSMO film and the PMN–PT substrate [insets (b) and (c) of Fig. 2, respectively], showing the epitaxial growth of the LCSMO film on the PMN–PT substrate.

The inset in Fig. 3 shows the temperature dependence of the resistivity and magnetization for the LCSMO/PMN–PT structure without Terfenol-D. With decreasing temperature, the film undergoes an insulator-to-metal transition near $T_p \sim 220$ K, which coincides with the onset temperature of the paramagnetic (PM) to ferromagnetic (FM) phase transition. Measurements of magnetic hysteresis loops at various fixed temperatures indicate that the film is in PM state for $T \geq 220$ K but in FM state for $T < 220$ K (see Fig. 3).

To observe the strain effects induced by the magnetostriction of the Terfenol-D alloy, we measured the MR of the LCSMO film at several fixed temperatures ranging from the FM state to the PM state for the LCSMO/PMN–PT structure without Terfenol-D. Here, the PMN–PT substrate was in the unpoled state and the MR is defined as $MR = [\rho(H) - \rho(0)]/\rho(0)$ where $\rho(0)$ and $\rho(H)$ are the resistivity of the film in zero magnetic field and a magnetic field H, respectively. It should be noted that the direction of the magnetic field was perpendicular to the film plane. The MR versus H curves at T = 80, 150, 220, and 250 K are presented in Fig. 4. Similar to that observed in the $La_{0.7}Ba_{0.3}MnO_3$/PMN–PT structure [14], the MR of the LCSMO film shows a maximum near T_P (~220 K). After measuring the values of MR versus H for the LCSMO/PMN–PT structure, the exact same piece of LCSMO/PMN–PT structure was bonded to a 10 mm × 5 mm × 1 mm Terfenol-D plate using electrically conductive silver loaded epoxy (E-Solder™ 3022, Von Roll Isola, USA) and the MR of the LCSMO film for the LCSMO/PMN–PT/Terfenol-D structure was again measured at T = 80, 150, 220, and 250 K, respectively. The direction of the magnetic field was also perpendicular to the film plane so that the Terfenol-D plate generates an in-plane compressive strain due to the magnetostriction. Interestingly, once the LCSMO/PMN–PT structure was bonded to the Terfenol-D plate, the MR of the film changed significantly. It is worth mentioning that the MR in the PM state (e.g., T = 220 and 250 K) is enhanced while the MR in the FM state (e.g., T = 80 and 150 K) is reduced, when comparing the MR values of the LCSMO/PMN–PT structure without Terfenol-D. In other words, the MR shows opposite changes in the PM state and the FM state in a magnetic field after the LCSMO/PMN–PT structure had been bonded to a Terfenol-D plate. Since, the PMN–PT substrate was in the unpoled state for the LCSMO/PMN–PT/Terfenol-D structure, there would be no piezoelectric effect (i.e. no elec-

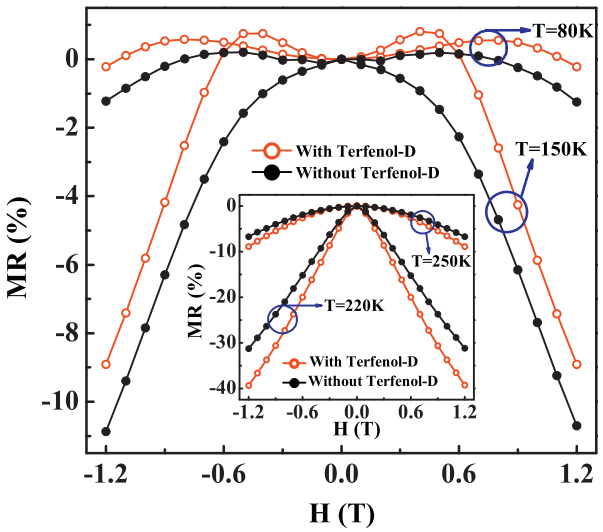

Fig. 4. MR of the LCSMO film for the LCSMO/PMN–PT structure and the LCSMO/PMN–PT/Terfenol-D structure measured at $T = 80$, 150, 220, and 250 K, respectively.

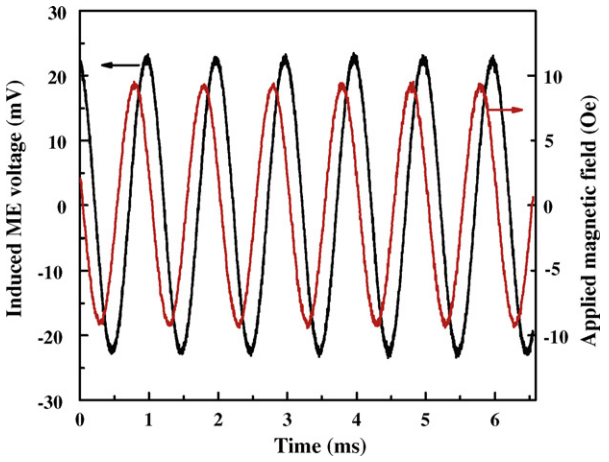

Fig. 5. ME voltages induced by a sinusoidal ac magnetic field with a peak value 9.1 Oe as a function of time at a frequency of 1 kHz.

tric charge was induced at the interface between the film and the PMN–PT substrate) in the LCSMO/PMN–PT/Terfenol-D structure when a dc magnetic field is applied. Therefore, the change of MR could not be caused by the ME effect. We note that the MR–H curves at $T = 80$ and 150 K show peaks at $H = 0.75$ and 0.5 T, respectively, which may be due to the result of anisotropic MR effect that is often observed in the FM state when a magnetic field is applied perpendicular to the plane of a manganite thin film [15,16].

It is well known that Terfenol-D is a magnetostrictive material. When a magnetic field is applied perpendicular to the plane of the Terfenol-D plate, the magnetic domains would rotate toward the direction of the magnetic field, producing an out-of-plane tensile strain and an in-plane compressive strain. The induced in-plane compressive strain is then transferred to the PMN–PT substrate (which has been widely observed in PMN–PT/Terfenol-D laminate structures [6–9,11]). Thus, the PMN–PT substrate would be biaxially compressed in the in-plane direction, which is believed to reduce the in-plane tensile strain of the LCSMO film since, the film is epitaxially grown on the PMN–PT substrate. To verify whether the strain induced by the magnetostriction of the Terfenol-D plate has been effectively transferred to the PMN–PT or not, we poled the PMN–PT substrate and measured the ME effects of the LCSMO/PMN–PT/Terfenol-D structure. Before measuring the induced ME voltages between the top gold electrode and the bottom Terfenol-D, a dc bias field of $H_{dc} = 2500$ Oe was applied perpendicular to the plane of the Terfenol-D plate. Fig. 5 shows the ME voltages induced by a sinusoidal ac magnetic field with a peak value 9.1 Oe as a function of time at a frequency of 1 kHz. The ME voltages were sinusoidally modulated at the same frequency as the driving ac magnetic field. The ME coefficient α_E was calculated to be ~65.6 mV/cm Oe. We also measured the ME voltages as a function of time when the same sinusoidal ac magnetic field was applied parallel to the plane of the Terfenol-D plate under a dc bias field of $H_{dc} = 400$ Oe and found a ME coefficient $\alpha_E \sim 289.2$ mV/cm Oe (results are not shown here). Therefore, the appearance of the ME effects in the LCSMO/PMN–PT/Terfenol-D structure indicates that the strain induced by the magnetostriction of the Terfenol-D plate has been transferred to the PMN–PT substrate. Here, we note that the value of the strain transferred to the PMN–PT substrate is related to the thickness of the Terfenol-D plate. It is expected that the thinner the Terfenol-D plate, the smaller the strain is transferred to the PMN–PT substrate, and thus causing a smaller change in MR.

The effects of the strain induced by the magnetostriction on MR can be explained in terms of coexisting phases whose volume fractions are altered as a result of the strain induced by the magnetostriction of the Terfenol-D. For perovskite manganites showing an insulator-to-metal transition, the FM metallic phase strongly competes with the PM insulating phase near the insulator-to-metal transition temperature T_P where a maximal MR is often observed. The ratio of the volume fractions of the FM metallic phase (f_{FM}) to that of the PM insulating phase ($1 - f_{FM}$) has an optimal value $\lambda_{optimal}$ near T_P. It has been observed that, whether the value of $f_{FM}/(1 - f_{FM})$ is larger or smaller than $\lambda_{optimal}$, MR decreases due to reduced competition between the FM metallic phase and the PM insulating phase [12,14]. In the PM state ($T \geq 220$ K), because of the local Mn^{3+}–O–Mn^{4+} double exchange interaction, a small fraction of FM metallic phase is embedded in the PM insulating matrix, resulting in $f_{FM}/(1 - f_{FM}) < \lambda_{optimal}$ in the PM state. Associated with the reduction in the in-plane tensile strain in the LCSMO film induced by the magnetostriction of Terfenol-D, the tetragonal distortion of the MnO_6 octahedra of the film would be reduced, as revealed by the angular resolved X-ray absorption spectroscopy by Souza-Neto et al. [17]. Such a decrease in the tetragonal distortion of the MnO_6 octahedra weakens the electron-lattice coupling strength and increases the double-exchange interaction, thereby favoring the active hopping of e_g electrons [18–20]. This leads to the volume fraction of FM metallic phase to increases at the expense of the PM insulating phase [12]. Consequently, the value of $f_{FM}/(1 - f_{FM})$ in the PM state becomes larger and closer to $\lambda_{optimal}$. The MR is, thus, enhanced due to enhanced phase separation. However, in the FM state (e.g. $T = 80$ K), the FM metallic phase already dominates over the PM insulating phase, i.e. $f_{FM}/(1 - f_{FM}) > \lambda_{optimal}$, the magnetostriction-induced increase in f_{FM} and decrease in $(1 - f_{FM})$ cause the value of $f_{FM}/(1 - f_{FM})$ to be even larger than $\lambda_{optimal}$. The MR is, thus, reduced due to reduced phase separation. Therefore, the different responses of the MR to the magnetostriction-induced strain in the PM state and FM state could be explained by the strain-induced modification in the phase separation.

4. Conclusions

We modify the strain and MR of the LCSMO film in the LCSMO/PMN–PT/Terfenol-D structure via the magnetostriction of Terfenol-D alloy. The magnetostriction induces an in-plane compressive strain which is transferred to the PMN–PT substrate and is, thus, believed to reduce the tensile strain of the LCSMO film.

Consequently, MR of the film shows opposite changes in the paramagnetic and ferromagnetic states and these changes are explained in terms of coexisting phases whose volume fractions are modified due to the reduction in the tetragonal distortion of MnO_6 octahedra and enhancement of double-exchange interaction. The method of dynamic modification of film strain using magnetostriction opens a new pathway to study the intrinsic strain effects of complex oxide thin films (particularly for nonmagnetic thin films) without introducing certain effects brought by extrinsic variables, which are often present in previous methods based on comparing properties of a set of thin films with different thicknesses.

Acknowledgments

This work was supported by the Hong Kong Research Grants Council under grant no. CERG PolyU 5122/07E, and the Center for Smart Materials of the Hong Kong Polytechnic University.

References

[1] P. Orgiani, A. Guarino, C. Aruta, C. Adamo, A. Galdi, A.Yu. Petrov, R. Savo, L. Maritato, J. Appl. Phys. 101 (2007) 033904.
[2] R. Werner, C. Raisch, V. Leca, V. Ion, S. Bals, G.V. Tendeloo, T. Chasse, R. Kleiner, D. Koelle, Phys. Rev. B 79 (2009) 054416.
[3] S. Liang, J.R. Sun, J. Wang, B.G. Shen, Appl. Phys. Lett. 95 (2009) 182509.
[4] D. Lee, H.S. Kim, S.Y. Jang, K.W. Joh, T.W. Noh, J. Yu, C.E. Lee, J.-G. Yoon, Phys. Rev. B 81 (2010) 012101.
[5] K. Daoudia, T. Tsuchiyab, T. Nakajimab, A. Fouzric, M. Oueslatia, J. Alloys Compd. 506 (2010) 483.
[6] Y.J. Wang, X.Y. Zhao, J. Jiao, L.H. Liu, W.N. Di, H.S. Luo, S.W. Or, J. Alloys Compd. 500 (2010) 224.
[7] Y.J. Wang, X.Y. Zhao, W.N. Di, H.S. Luo, S.W. Or, Appl. Phys. Lett. 95 (2009) 143503.
[8] Y.J. Wang, C.M. Leung, F.F. Wang, S.W. Or, X.Y. Zhao, H.S. Luo, J. Phys. D: Appl. Phys. 42 (2009) 135414.
[9] Y.J. Wang, C.M. Leung, S.W. Or, X.Y. Zhao, H.S. Luo, J. Alloys Compd. 487 (2009) 450.
[10] H.S. Luo, G.S. Xu, H.Q. Xu, P.C. Wang, Z.W. Yin, Jpn. J. Appl. Phys. 1 (39) (2000) 5581.
[11] Y.J. Wang, S.W. Or, H.L.W. Chan, X.Y. Zhao, H.S. Luo, J. Appl. Phys. 103 (2008) 124511.
[12] R.K. Zheng, H.-U. Habermeier, H.L.W. Chan, C.L. Choy, H.S. Luo, Phys. Rev. B 80 (2009) 104433.
[13] B. Noheda, D.E. Cox, G. Shirane, J. Gao, Z.-G. Ye, Phys. Rev. B 66 (2002) 054104.
[14] R.K. Zheng, Y. Jiang, Y. Wang, H.L.W. Chan, C.L. Choy, H.S. Luo, Phys. Rev. B 79 (2009) 174420.
[15] H.S. Wang, Q. Li, Appl. Phys. Lett. 73 (1998) 2360.
[16] H.S. Wang, Q. Li, Appl. Phys. Lett. 74 (1999) 2212.
[17] N.M. Souza-Neto, A.Y. Ramos, H.C.N. Tolentino, E. Favre-Nicolin, L. Ranno, Phys. Rev. B 70 (2004) 174451.
[18] A.J. Millis, T. Darling, A. Migliori, J. Appl. Phys. 83 (1998) 1588.
[19] X.J. Chen, S. Soltan, H. Zhang, H.-U. Habermeier, Phys. Rev. B 65 (2002) 174402.
[20] X.J. Chen, H.-U. Habermeier, H. Zhang, G. Gu, M. Varela, J. Santamaria, C.C. Almasan, Phys. Rev. B 72 (2005) 104403.